JOURNAL OF PHYSICAL ORGANIC CHEMISTRY
J. Phys. Org. Chem. 2002; **15:** 524–528
Published online in Wiley InterScience (www.interscience.wiley.com). DOI: 10.1002/poc.522

Mechanism of hydrogen abstraction from methane and hydrofluoromethanes by hydroxyl radical†

Jacek Korchowiec*

K. Gumiński Department of Theoretical Chemistry, Faculty of Chemistry, Jagiellonian University, R. Ingardena 3, 30-060 Cracow, Poland

Revised 30 January 2002; accepted 15 February 2002

ABSTRACT: The self-consistent charge and configuration method for subsystems (SCCCMS) is applied to discuss the mechanism of hydrogen abstraction from methane and hydrofluoromethanes by hydroxyl radicals. All calculations are done at the B3LYP level of theory with the 6–311G(d,p) basis set. The results of energy partitioning, performed for transition-state structures and two additional points on the minimum energy paths, demonstrate that the perturbation in the external potential (due to nuclei), namely classical/non-classical electrostatic and polarization energies, is the most important. The formation of a pre-reaction molecular adduct is controlled by electrostatic interactions due to their long-range character. The charge-transfer energy is unimportant for the hydrogen abstraction reactions. Copyright © 2002 John Wiley & Sons, Ltd.

KEYWORDS: chemical reactivity; energy partitioning schemes; hydrogen abstraction reaction; hydrofluorocarbons

INTRODUCTION

Halons (bromofluorocarbons) and Freons (chlorofluorocarbons) were used as refrigerants, foam blowing substances and aerosol spray propellants. Unfortunately, these compounds have a strong impact on ozone depletion in the stratosphere.[1,2] The free radicals, namely, chlorine and bromine atoms with relatively long lifetimes, produced during the photolysis, catalyze the destruction of stratospheric ozone. Such very undesirable behavior caused both groups of substances to be withdrawn from commercial use.

Hydrofluorocarbons (HFCs) were designed as possible replacements of fully halogenated species. These 'environmentally friendly' compounds (HFCs are man-made 'greenhouse' gases and have an impact on the radiative balance of the Earth) are removed from the troposphere. The first step in the degradation of HFCs is hydrogen abstraction by ·OH radical. This paper reports theoretical investigations of the mechanism of hydrogen abstraction from methane and its fluoro derivatives by ·OH radical:

$$CH_{4-n}F_n + {}^{\cdot}OH \rightarrow {}^{\cdot}CH_{3-n}F_n + H_2O \qquad (1)$$

where $n = 0$, 1, 2 or 3. Methane, the fluorine-free parent molecule, is a natural greenhouse gas, so all the reactants in Eqn. (1) are of great importance in atmospheric chemistry. For these reasons, it is not surprising that many experimental[3–6] and theoretical[7–15] studies have been carried out. The previous theoretical studies have indicated that large basis sets and high levels of treatment of electron correlation are required for an adequate description of the kinetics and energetics for $CH_4/{}^{\cdot}OH$[12–23] and the remaining systems.[12–15]

The main goal of the present analysis is to explain the mechanism of reaction (1). The previous investigations concentrated on the temperature dependence of rate constants and on activation energies. Hence the molecular electronic mechanism of the hydrogen abstraction was not exactly addressed. Here, we will try to solve this problem by means of an energy partitioning technique. The system interaction energy will be decomposed into electrostatic, exchange, charge-transfer, polarization and deformation contributions for previously located transition-state structures[14] and two additional points on the minimum energy paths.

COMPUTATIONAL METHODOLOGY

The interaction energy is decomposed using the self-consistent charge and configuration method for subsystems (SCCCMS).[24,25] This scheme follows hypothetical stages of charge reorganization during the course of reaction. On going from isolated (non-interacting) species (*i*) to reactants in a molecular complex (*iv*), one has to distinguish additionally rigid (*ii*) and polarized (*iii*)

**Correspondence to:* J. Korchowiec, K. Gumiński Department of Theoretical Chemistry, Faculty of Chemistry, Jagiellonian University, R. Ingardena 3, 30-060 Cracow, Poland.
E-mail: korchow@chemia.uj.edu.pl
†Presented at the 8th European Symposium on Organic Reactivity (ESOR-8), Cavtat (Dubrovnik), Croatia, September 2001.
Contract/grant sponsor: Committee for Scientific Research in Poland; *Contract/grant number:* 3 T09A 141 19.

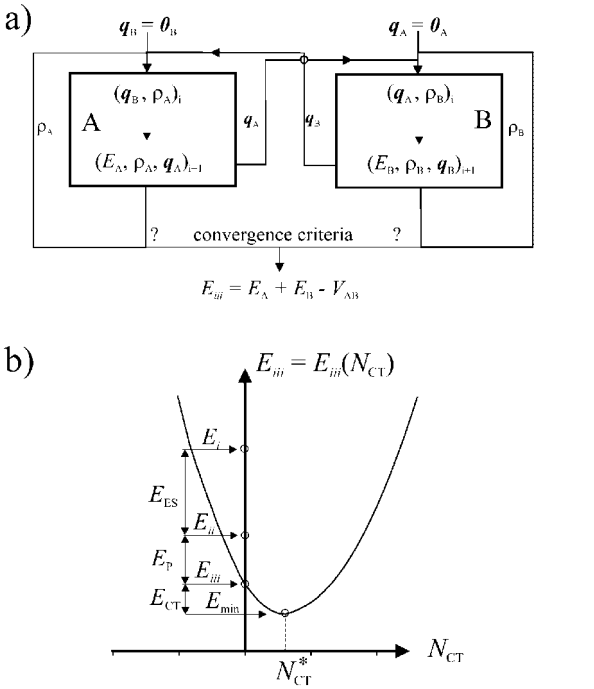

Figure 1. (a) Scheme illustrating the SCCCMS procedure and (b) qualitative cut of the energy surface in the population space $E_{iii} = E_{iii}(q_A, q_B)$ along the isoelectronic line: $dq_A = -dq_B = q_{CT} = -N_{CT}$. Energies E_i, E_{ii} and E_{iii} correspond to the system at initial and intermediate stages in the charge reorganization. The optimum amount of charge transferred from B to A is denoted N^*_{CT}

reactants. Both intermediate steps, and also the final one (*iv*), describe interacting subsystems. In step *ii*, electron densities are exactly the same as in step *i*, so the calculations are performed for frozen (rigid) interacting species. In step *iii*, electron densities of reactants are allowed to relax and the only constraint is that subsystems are closed to each other. In other words, charge transfer between subsystems is forbidden. Finally, in step *iv*, there are no constraints (open reactants in molecular complex). Steps *i* and *iv* correspond to quantum-mechanical calculations for reactants and supermolecule, respectively. The intermediate steps *ii* and *iii* are modeled by SCCCMS calculations.

In the SCCCMS scheme, the presence of the reaction partner is approximated by its charge distribution. Calculations for reactant A (an acid) are performed with background charges of B (a base), $\boldsymbol{q}_B = \{q_1^B, q_2^B, \ldots\}$. Similarly, calculations for B are performed with background charges of A, $\boldsymbol{q}_A = \{q_1^A, q_2^A, \ldots\}$.This procedure is shown schematically in Fig. 1(a). Independent calculations are carried out for both reactants. The modified electron densities (ρ_A, ρ_B) and charge distributions ($\boldsymbol{q}_A$, $\boldsymbol{q}_B$) are the input data for the next iteration. The final iteration corresponds to mutually polarized reactants. The initial conditions are chosen in such a way that steps *i* and *ii* are naturally included in the computational scheme. Except for the first iteration, where $\boldsymbol{q}_A = \boldsymbol{0}_A$ and $\boldsymbol{q}_B = \boldsymbol{0}_B$, the energy of the whole system is not an additive quantity: $E_{iii} \neq E_A + E_B$. The additional component V_{AB} should be introduced in order to eliminate electrostatic interactions that are doubly counted.

A single SCCCMS run is required to obtain electrostatic (ES) and polarization (P) energies:

$$E_{ES} = E_{ii} - E_i \tag{2}$$

$$E_P = E_{iii} - E_{ii} \tag{3}$$

The difference $E_{iv} - E_{iii}$ combines exchange-repulsion (EX) and charge-transfer (CT) energies. Further partitioning can be done after constructing an energy surface in the population space $E_{iii} = E_{iii}(q_A, q_B)$, where $q_A = \sum_{\alpha \in A} q_\alpha^A$ and $q_B = \sum_{\beta \in B} q_\beta^B$ are the overall charges of A and B, respectively. The cut $E_{iii} = E_{iii}(N_{CT})$ along the isoelectronic line $dq_A = -dq_B = dq_{CT} = -N_{CT}$ (preserving number of electrons in the whole system) is shown in Fig. 1(b). The energies E_i, E_{ii} and E_{iii} obtained for the reference system ($N_{CT} = 0$, e.g. neutral reactants) are plotted as open circles. By definition, $E_{iii} - E_{ii}$ is less than zero. There is no restriction for the location of E_i, so the difference $E_{ii} - E_i$ can be either positive or negative. The energy lowering $E_{min} - E_{iii}$ defines the CT energy. Now, the EX energy is obtained from the balance equation:

$$E_{EX} = E_{iv} - E_{iii} - E_{CT} \tag{4}$$

Note that the minimum on the energy curve of Fig. 1(b) does not correspond to the energy of the supermolecule since SCCCMS works within the polarization approximation. At the Hartree–Fock (HF) level of theory, E_{EX} is dominated by exchange-repulsion interactions, although it also includes part of the electrostatic energy (higher order terms from the multipole expansion) due to the approximate character of SCCCMS calculations. At the post-HF and density functional level of theory, it also includes inter-reactant correlation energy (dispersion energy). In steps *i*–*iv*, reactant geometries are fixed and are the same as in the combined system. This guarantees that the external potential (due to nuclei) is constant. Since the geometries of reactants in the supermolecule are different from those of reactants in the minimum energy structure, one has to define the geometry deformation (DEF) contribution to the interaction energy:

$$E_{DEF} = E_i^0 - E_i \tag{5}$$

The superscript 0 denotes that every reactant has the most stable configuration. Of course, all the above terms sum to the global (g) interaction energy, $E_{ES} + E_{EX} + E_{CT} + E_P + E_{DEF} = E_{INT} + E_{DEF} \equiv E_g$. For more detail, see Refs 24 and 25.

All calculations, including SCCCMS calculations, were carried out using the Gaussian 98 suite of

programs.[26] The B3LYP hybrid functional,[27] i.e. the combination of the Becke's 1988 exchange functional[28] with HF exchange and the correlation functional of Lee, Yang and Parr,[29,30] was used in the Kohn–Sham scheme. The 6–311G(d,p) basis set[31,32] was employed. Energy decomposition was performed for transition-state geometries and two additional points on the minimum energy path, i.e. $r = 1.9$ and 2.3 Å; as the reaction coordinate (r) we used the distance between the hydrogen atom from the $CH_{4-n}F_n$ molecule and the oxygen atom from the radical: $F_nH_{3-n}CH\overset{r}{\cdots}OH$. The electrostatically derived charges were employed in the SCCCMS scheme. The energy surface in the population space (the cubic function) was constructed from 16 points (the global subsystem charge was changed from −1 to +2).

RESULTS AND DISCUSSION

The components of interaction energy obtained at the B3LYP level of theory are collected in Table 1 and shown in Fig. 2. A negative (positive) sign indicates a stabilizing (destabilizing) contribution. By definition, CT and P energies should stabilize the system, whereas DEF energy should destabilize the system. This is indeed reflected by the numerical values given in the table. The EX component at the HF level of theory is usually destabilizing for two closed-shell molecules. Here, one of the subsystems is a radical (open-shell system). Moreover, at the DFT level of theory this energy term also includes dispersion energy. The repulsive character of EX energy is stressed at shorter separations. The ES energy can be either positive or negative.

The chemical process can be seen as a perturbation either in the number of electrons $dN = dN_A + dN_B$ or in the external potential due to nuclei $d\nu(\vec{r}) = d\nu_A(\vec{r}) + d\nu_B(\vec{r})$. Note that the variables N_A and $\nu_A(\vec{r})$ [N_B and $\nu_B(\vec{r})$]uniquely define the hamiltonian of reactant A (B). Changes in the system energy can be approximated by Taylor expansion:

$$dE = \left(\frac{\partial E}{\partial N}\right)dN + \int\left(\frac{\delta E}{\delta\nu(\vec{r})}\right)d\nu(\vec{r})d\vec{r} + \frac{1}{2}\left(\frac{\partial^2 E}{\partial N^2}\right)(dN)^2 + \frac{1}{2}\int\left(\frac{\delta^2 E}{\delta\nu(\vec{r})\delta\nu(\vec{r}')}\right)d\nu(\vec{r})d\nu(\vec{r}')d\vec{r}d\vec{r}' + \int\left(\frac{\delta}{\delta\nu(\vec{r})}\frac{\partial E}{\partial N}\right)d\nu(\vec{r})d\vec{r}dN + \cdots \quad (6)$$

The relevant expression in the reactant resolution can be obtained after introducing chain rule transformations $\partial/\partial N = \sum_X (\partial/\partial N_X)(\partial N_X/\partial N)$ and $\delta/\delta v(\vec{r}) = \sum_X \int d\vec{r}[\delta/\delta\nu_X(\vec{r}')][\delta\nu_X(\vec{r}')/\delta\nu(\vec{r})]$, where X = A and B, into Eqn. (6).[33] In such a perturbative description, ES and EX are the first-order classical and non-classical contributions in $d\nu$, P is the second-order contribution in $d\nu$ and CT contains first- and second-order contributions in dN, as well as the mixed $dNd\nu$ second-order contribution. In the SCCCMS procedure calculations for A and B are carried out separately, so $d\nu_A(\vec{r})$ and $d\nu_B(\vec{r})$ are approximated by the effective electrostatic potentials of the reaction partners. The perturbations $dN_A = -dq_A$ and $dN_B = -dq_B$ are modeled by different oxidation/reduction states of reactants.

All energy components should disappear with increasing r. Figure 2 illustrates such behavior; however, the CT energy is slightly higher for $r = 2.3$ Å than for $r = 1.9$ Å. It seems that the CT energy reaches an unphysical asymptotic value owing to a too-small subsystems coupling.[33] Note that this term is almost equal to zero for $r = 1.9$ Å, hence the additional stabilization should be put in EX energy since it is computed by the balance equation. The sharpest decrease is seen for DEF energy. This is the only contribution to E_g that can be separated into reactant contributions. In the case of $CH_{4-n}F_n$/·OH

Table 1. Decomposition of the interaction energy for CH_4/·OH, CH_3F/·OH, CH_2F_2/·OH, and CHF_3/·OH systems at the B3LYP/6–311(d,p) level of theory[a]

System	r	E_{DEF}	E_{ES}	E_P	E_{CT}	E_{EX}	E_{INT}
CH_4/·OH	1.29	6.4	−2.5	−1.9	−1.6	2.2	2.6
	1.90	0.1	−1.0	−0.4	−0.0	0.6	−0.7
	2.30	0.0	−0.3	−0.0	−0.4	−0.2	−1.0
CH_3F/·OH	1.36	3.6	−4.0	−1.8	−1.7	2.9	−0.9
	1.90	0.1	−3.3	−0.0	−0.0	−0.3	−3.4
	2.30	0.3	−3.9	−0.6	−0.1	−1.1	−5.4
CH_2F_2/·OH	1.37	3.0	−5.1	−1.5	−0.8	3.1	−1.3
	1.90	0.1	−3.1	−1.1	−0.2	1.5	−2.8
	2.30	0.0	−1.9	−0.2	−0.3	0.2	−2.2
CHF_3/·OH	1.27	6.4	−5.8	−3.1	−1.2	5.4	1.6
	1.90	0.1	−3.2	−1.1	−0.0	2.2	−2.1
	2.30	0.1	−1.3	−0.0	−0.1	−0.4	−1.7

[a] All energies are in kcal mol^{-1}, (1 kcal = 4.184 kJ) and the reaction coordinate r is in Å. The first row for each molecular system entry corresponds to the transition-state geometry.

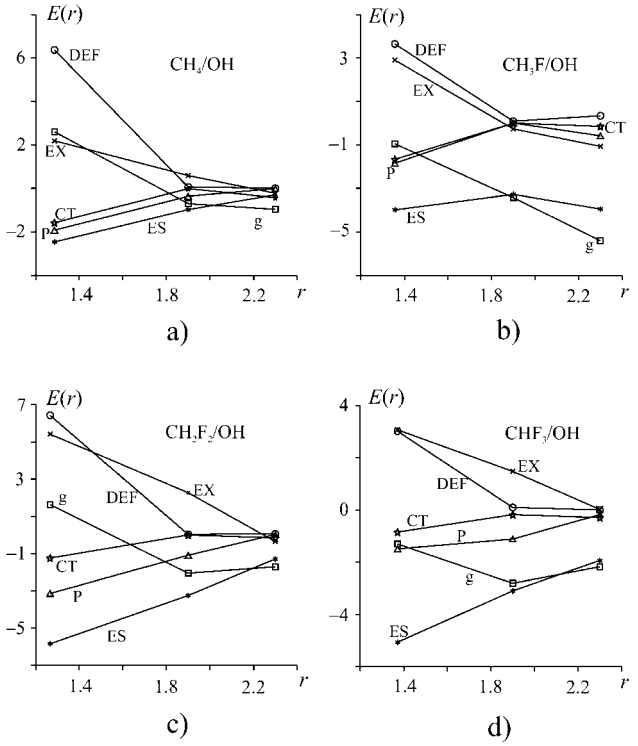

Figure 2. Dependence of global interaction energy and its components on the mutual separation between hydroxyl radical and (a) methane, (b) fluoromethane, (c) difluoromethane and (d) trifluoromethane. Lines connecting points are for clarity

systems, almost 100% of the deformation comes from methane or hydrofluoromethane (stretching of C—H bond). Thus, the shorter is r, the greater is E_{DEF}.

The global interaction energies for all systems and inter-reactant separations are listed in the last column of Table 1. The negative values of E_g for $CH_3F/^{\cdot}OH$ and $CH_2F_2/^{\cdot}OH$ in transition-state structures are indicators of stable pre-reaction molecular adducts. For the remaining two systems, $CH_4/^{\cdot}OH$ and $CHF_3/^{\cdot}OH$, such complexes also exist (negative values of E_g for other points on the minimum energy path). The presence of such van der Waals-type complexes can be attributed to electrostatic stabilization. The most important interatomic interaction is between the hydrogen atom from $CH_{4-n}F_n$ (positive partial charge) and the oxygen from $^{\cdot}OH$ (negative charge). In fluorinated systems, there is additional stabilization due to F···H interaction (negative partial charge on fluorine atom and positive on H atom).

The structures of pre-reaction adducts have been recently located by El-Taher at the UHF 6-31G* level of theory.[34] Hydroxyl radical combines with fluoromethanes through a hydrogen bonding either from the H atom of $^{\cdot}OH$ to a fluorine atom of F_nCH_{4-n} ($^{\cdot}OH\cdots F_nCH_{4-n}$) or from the O atom of $^{\cdot}OH$ to a hydrogen atom of $H_{4-n}F_nC$ ($HO^{\cdot}\cdots H_{4-n}F_nC$). The former adducts are lower in energy than the latter. For $CH_4/^{\cdot}OH$ only one adduct appears. The energy surface for hydrogen abstraction reaction is very flat. Hence it is especially difficult to locate $HO^{\cdot}\cdots HCH_{3-n}F_n$ adducts. We have done this in an approximate way by freezing the geometries of reactants. The inter-reactant separations obtained are 2.21 Å ($CH_4/^{\cdot}OH$), 2.04 Å ($CH_3F/^{\cdot}OH$), 2.43 Å ($CH_2F_2/^{\cdot}OH$) and 2.27 Å ($CHF_3/^{\cdot}OH$).

The most important stabilizing contribution to E_g is the ES component. Figure 2 underlines the long-range character of electrostatic energy (very slow decrease to an asymptotic value). In the case of fluorinated systems, the g and ES curves are very close to each other for long and intermediate separations ($r = 2.3$ and 1.9 Å). Hence the formation of the pre-reaction molecular adduct is an ES-controlled process. In the case of $CH_4/^{\cdot}OH$, the formation of the molecular adduct can also be connected with electrostatic interactions since the EX energy, due to the approximate character of the SCCCMS scheme, contains higher order terms from distributed multiple expansion. At shorter distances, this picture changes, owing to larger DEF and EX energies.

The CT and P components are connected with the charge reorganization. Table 1 and Fig. 2 indicate that the energy lowering due to P is larger than that due to CT, except at $r = 2.3$ Å, where the differences are negligible. This picture of interaction is very close to that observed in other hydrogen-bonded systems.[25,35] For a large inter-reactant separation ($r = 2.3$ Å) both contributions are unimportant. For intermediate separation ($r = 1.9$ Å), except for $CH_3F/^{\cdot}OH$, the P energy is one order of magnitude higher than the CT energy. For transition-state geometries, the differences are less pronounced but still the P energy is more stabilizing than the CT energy. Hence charge reorganization due to P is greater than that due to CT.

Stabilizing contributions to E_{INT} increase in the order $|E_{\mathrm{CT}}| < |E_{\mathrm{P}}| < |E_{\mathrm{ES}}|$ for all systems and inter-reactant separations. Such behavior clearly indicates that the hydrogen abstraction is a dν process. The CT energy is more cosmetic. It is also reflected in the amount of charge transferred between interacting subsystems; electrons flow from the organic molecule to the hydroxyl radical and N^*_{CT} is not greater than 0.1.

For all systems, investigated the transition states are more reactant like.[13,14] In addition, the transition states for $CH_3F/^{\cdot}OH$ and $CH_2F_2/^{\cdot}OH$ are significantly earlier than those for $CH_4/^{\cdot}OH$ and $CHF_3/^{\cdot}OH$. This indicates that the fluorine substituent effect cannot be interpreted as a simple rule. However, for transition-state structures one can observe that the more fluorine atoms there are in the system, the greater is ES stabilization. Except for EX energy, no other components show such behavior. Thus only the first-order term in dν shows an 'additive' substituent effect on going from the $CH_4/^{\cdot}OH$ to the $CHF_3/^{\cdot}OH$ system.

Table 2 gives the reaction energies (ΔE) and barrier heights ($\Delta E\ddagger$) for the hydrogen abstraction reactions. All the reactions are exothermic, in agreement with experi-

Table 2. Reaction energies (ΔE) and barrier heights ($\Delta E\ddagger$) obtained at the B3LYP/6–311G(*d,p*) level of theory for the hydrogen abstraction from methane and hydrofluoromethanes by $^{\cdot}OH$ radical: $CH_{4-n}F_n + {}^{\cdot}OH \rightarrow {}^{\cdot}CH_{3-n}F_n + H_2O$, $n = 0$, 1, 2 and 3

Quantity	$n = 0$	$n = 1$	$n = 2$	$n = 3$
ΔE	−8.1	−13.9	−14.3	−9.4
$\Delta E\ddagger$	3.6	2.3	2.1	4.6

mental data. The barrier height $\Delta E\ddagger = E^{TS} - E^{adduct}$ (E^{TS} and E^{adduct} are the energies of transition state and pre-reaction adduct) decreases smoothly on going from the $CH_4/{}^{\cdot}OH$ to the $CH_2F_2/{}^{\cdot}OH$ system and then increases sharply and reaches the highest value for the $CHF_3/{}^{\cdot}OH$ system. Exactly the same behavior is seen in experimentally derived activation energies.[3,4] Thus, the fluorine substitution effect is correctly, qualitatively reproduced at the B3LYP/6–311G(*d,p*) level of theory. This suggests that the computational method, in addition to the basis set, were adequate for describing the electronic mechanism of the hydrogen abstraction from methane and hydrofluoromethanes by hydroxyl radical.

CONCLUSIONS

We have investigated the mechanism of hydrogen abstraction from methane and hydrofluoromethanes by hydroxyl radical. The energy partitioning technique was carried out for transition-state structures and two additional points on the minimum energy paths. The interaction energy was decomposed into deformation, electrostatic, exchange, polarization and charge-transfer contributions.

The results obtained indicate the formation of a pre-reaction molecular adduct. In fluorinated systems, adduct stabilization is attributed to electrostatic energy. For the fluorine-free parent system also, exchange energy that includes part of the electrostatic and dispersion contributions stabilizes molecular adduct.

The hydrogen abstraction reaction is mainly controlled by perturbation in the external potential. The perturbation in the charge-transfer variable is unimportant. The 'additive' fluorine-substituent effect is reflected only in first-order classical and non-classical electrostatic energies. Other components of the interaction energy do not show such a regular dependence.

Acknowledgements

This work was supported by a grant from the Committee for Scientific Research in Poland (Project No. 3 T09A 141 19). All calculations were performed in ACK CYFRONET AGH, supported by computational grant No. KBN/SGI_ORIGIN_2000/UJ/067/1999.

REFERENCES

1. Findlayson-Pitts B, Pitts JN. *Atmospheric Chemistry*. John Wiley: Chichester, 1986.
2. Pilling MJ, Seakins PW. *Reaction Kinetics*. Oxford University Press: New York, 1995.
3. Hsu KJ, DeMore WB. *J. Phys. Chem.* 1995; **99**: 1235–1244.
4. DeMore WB. *J. Phys. Chem.* 1996; **100**: 5813–5820.
5. Orkin VL, Huie RE, Kurylo MJ. *J. Phys. Chem. A* 1997; **101**: 9118–9124.
6. Ravishankara AR, Turnipseed AA, Jensen NR, Barone S, Mills M, Howard CJ, Solomon S. *Science* 1994; **263**: 71–75.
7. Cooper DL, Cunningham TP. *Atmos. Enviro.* 1992; **26A**: 1331–1334.
8. Martell JM, Boyd RJ. *J. Phys. Chem.* 1995; **99**: 13402–13411.
9. Martell JM, Tee JB, Boyd RJ. *Can. J. Chem.* 1996; **74**: 786–800.
10. Sekusak S, Gusten H, Sabljic A. *J. Phys. Chem.* 1996; **100**: 6212–6224.
11. Fu Y, Levis-Bevan W, Tyrrell J. *J. Phys. Chem.* 1995; **99**: 630–633.
12. Bottoni A, Poggi G, Emmi SS. *THEOCHEM* 1993; **279**: 299–309.
13. Jursic BS. *Chem. Phys. Lett.* 1996; **256**: 603–608.
14. Korchowiec J, Kawahara S, Matsumura K, Uchimaru T, Sugie M. *J. Phys. Chem. A* 1999; **104**: 3548–3553.
15. Schwartz M, Marshall P, Berry RJ, Ehlers CJ, Petersson GA. *J. Phys. Chem. A* 1998; **102**: 10074–10081.
16. Gonzales C, McDouall JJ. W.; Schlegel HB. *J. Phys. Chem.* 1990; **94**: 7467–7471.
17. Truong TN, Truhlar DG. *J. Chem. Phys.* 1990; **93**: 1761–1769.
18. Jones SAL, Pacey PD. *J. Phys. Chem.* 1992; **96**: 1764–1767.
19. Melissas VS, Truhlar DG. *J. Chem. Phys.* 1993; **99**: 1013–1027.
20. Melissas VS, Truhlar DG. *J. Chem. Phys.* 1993; **99**: 3542–3552.
21. Dobbs KD, Dixon DA, Komornicki A. *J. Chem. Phys.* 1993; **98**: 8852–8858.
22. Basch H, Hoz S. *J. Phys. Chem. A* 1997; **101**: 4416–4431.
23. Aliagas I, Gronert S. *J. Phys. Chem. A* 1998; **102**: 2609–2612.
24. Korchowiec J, Uchimaru T. *J. Phys. Chem. A* 1998; **102**: 6682–6689.
25. Korchowiec J, Uchimaru T. *J. Chem. Phys.* 2000; **112**: 1623–1633.
26. Frisch MJ, Trucks GW, Schlegel HB, Gill PMW, Johnson BG, Robb MA, Cheeseman JR, Keith T, Petersson GA, Montgomery JA, Raghavachari K, Al-Laham MA, Zakrzewski VG, Ortiz JV, Foresman JB, Cioslowski J, Stefanov BB, Nanayakkara A, Challacombe M, Peng CY, Ayala PY, Chen W, Wong MW, Andres JL, Replogle ES, Gomperts R, Martin RL, Fox DJ, Binkley JS, Defrees DJ, Baker J, Stewart JP, Head-Gordon M, Gonzalez C, Pople JA. Gaussian 98, Revision A.6. Gaussian: Pittsburgh, PA, 1998.
27. Becke AD. *J. Chem. Phys.* 1993; **98**: 5648–5652.
28. Becke AD. *Phys. Rev. A* 1988; **38**: 3098–3100.
29. Lee C, Yang W, Parr RG. *Phys. Rev. B* 1988; **37**: 785–789.
30. Miehlich B, Savin A, Stoll H, Preuss H. *Chem. Phys. Lett.* 1989; **157**: 200–206.
31. McLean AD, Chandler GS. *J. Chem. Phys.* 1980; **72**: 5639–5648.
32. Krishnan R, Binkley JS, Seeger R, Pople JA. *J. Chem. Phys.* 1980; **72**: 650–654.
33. Nalewajski RF, Korchowiec J. *Charge Sensitivity Approach to Electronic Structure and Chemical Reactivity*. Word Scientific: Singapore, 1997.
34. El-Taher S. *Int. J. Quantum Chem.* 2001; **84**: 426–440.
35. Mo Y, Gao J, Peyerimhoff SD. *J. Chem. Phys.* 2000; **112**: 5530–5538.